

# vGamba: Attentive State Space Bottleneck for efficient Long-range Dependencies in Visual Recognition

Yunusa Haruna  
Beihang University and NewraLab

Adamu Lawan  
Beihang University

## Abstract

Capturing long-range dependencies (LRD) efficiently is essential for visual recognition tasks, yet existing methods face limitations. Convolutional neural networks (CNNs) struggle with restricted receptive fields, while Vision Transformers achieve global context and LRD modeling at a high computational cost. State-space models (SSMs) offer an alternative, but adapting them into CNN-based bottlenecks is challenging, as it requires multiple architectural adjustments for visual processing. This work introduces vGamba, a simple yet effective hybrid vision backbone that integrates SSMs to enhance efficiency and representation learning. Its main component, the Gamba bottleneck, integrates the Gamba cell, an adaptation of Mamba for 2D spatial structures with positional awareness and an attentive spatial context (ASC) module. This design allows vGamba to leverage the computational efficiency of SSMs while maintaining high accuracy in modeling LRD. Extensive qualitative and quantitative experiments demonstrate that vGamba achieves superior performance in capturing LRD and outperforms several state-of-the-art models on downstream vision tasks.

## 1. Introduction

Modeling long-range dependencies (LRD) is essential in visual recognition for interpreting complex scenes where objects span large spatial regions, such as in instance segmentation or aerial imagery. Traditional convolutional neural network (CNN) backbones have dominated the field [3, 12, 24, 27, 28], and while their hierarchical structure allows effective feature extraction, their strong inductive bias and local receptive fields (RF) limit their ability to model LRD. To mitigate this, larger kernels and dilated convolutions have been used to expand the RF; however, larger kernels are computationally expensive, and dilation causes spatial discontinuities that reduce smooth LRD modeling [6, 34]. Consequently, Vision Transformers (ViT) [7] have

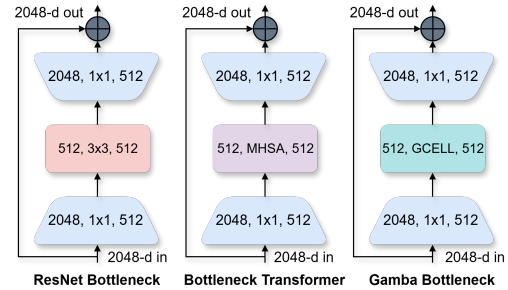


Figure 1. Bottleneck evolution from CNN based, ViT, and SSM

gained popularity for their ability to capture LRD using self-attention (SA) mechanisms, which allow them to model global context more effectively than CNN, Fig. 2. However, the computational cost of SA scales quadratically with sequence length, making ViT computationally expensive, especially for high-resolution images and real-time applications. Various techniques, such as low-rank factorization [33], linear approximation [20, 25], and sparse attention [2], have been proposed to reduce computational costs while preserving performance. However, these approaches often involve trade-offs between efficiency and effectiveness.

State-space models (SSM) [10] have recently emerged as an alternative to SA mechanisms, offering a more efficient way to model LRD. By capturing sequential dynamics in a compact form, SSMs reduce computational overhead while maintaining competitive performance. Mamba [9], a selective SSM, was introduced to further optimize efficiency, achieving up to 4-5 $\times$  higher throughput on sequence modeling benchmarks by selectively retaining relevant information and reducing redundant computations. However, adapting SSM for vision tasks remains challenging, as it requires specific spatial pre-processing. For instance, Vmamba [16] used a cross-scan and merging strategies to generate four directional SSM layers, while ViM [36] introduces bi-directional SSM that process information forward and backward. Although effective, these approaches increase architectural complexity and computational cost.

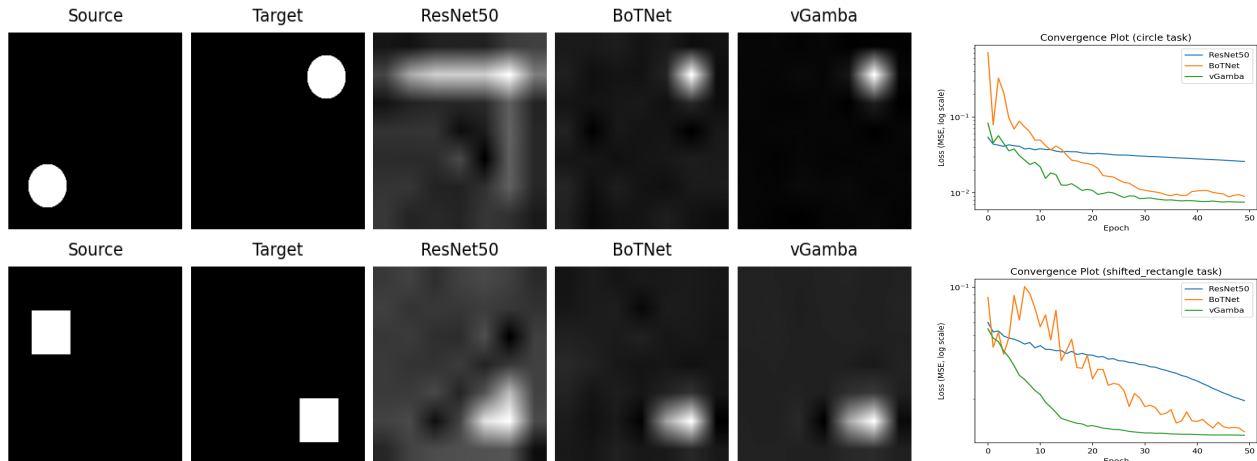


Figure 2. To test the models’ ability to capture LRD, we transport information between distant spatial diagonal locations, placing the source and target in opposite corners using different shapes. We compare three bottleneck architectures ResNet-50 (CNN), BoTNet (Transformer), and vGamba (SSM) all trained under identical settings (AdamW, lr 0.001, 50 epochs,  $224^2$ , MSE). ResNet-50 shows an almost straight-line convergence curve, indicating limited capacity to model LRD. In contrast, vGamba converges faster and more smoothly, producing more accurate reconstructions than ResNet-50 and BoTNet, effectively capturing LRD and spatial transport patterns.

To this end, we introduce vGamba, inspired by the Transformer bottleneck[26], we design a lightweight bottleneck module that integrates into the final layer of ResNet to efficiently capture LRD through a single SSM block. vGamba is a hybrid vision backbone built upon the Gamba Block, a compact structure derived from CNN bottlenecks. The Gamba cell extends Mamba for vision tasks by adapting it to 2D spatial structures and integrating ASC for enhanced spatial awareness. By combining these components, vGamba improves representational efficiency and contextual understanding, serving as an efficient alternative to conventional vision backbones.

The contributions of this work are summarized below:

- Existing SSM-based vision models require complex pre-processing and multi-SSM stacking, limiting integration into CNN-based bottlenecks. We address this gap with a lightweight, plug-and-play SSM bottleneck for ResNet.
- We introduce the Gamba bottleneck, a novel bottleneck structure that seamlessly integrates Mamba to enhance LRD modeling in visual recognition tasks.
- Experimental results on classification, detection, and object segmentation tasks demonstrate that vGamba outperforms several existing models, due to its enhancements in capturing global context and LRD.

## 2. Related Work

Efforts to capture LRD in visual data have evolved across several paradigms. Early CNN-based approaches focused on enlarging the RF by using larger kernels or dilated convolutions. For instance, the Global Convolutional Network [23] used large kernels to model LRD, while the

Dilated Residual Network [34] leveraged dilation to expand the RF without increasing model depth or complexity. While both approaches are effective, the former increases computational cost, whereas the latter can introduce gridding artifacts. An alternative is the Non-Local Neural Network [30], which mitigates this by computing responses as weighted sums over all positions, effectively capturing spatial-temporal LRD, but at high computational cost.

Building on this direction of global modeling, ViT [7] modeled global context from the first layer, treating image patches as tokens and linking them through SA, effectively capturing LRD. However, their quadratic complexity and large data demands make them resource-intensive. Several works addressed this: EfficientFormer [33] reduced backpropagation cost via low-rank projections, while LUNA [20] and UFO-ViT [25] proposed linear variants. SparseViT [2] further improved efficiency by pruning inactive tokens. Despite these advances, SA-based models remain costly for high-resolution visual tasks.

More recently, Mamba [9] applied SSMs to sequence modeling, offering efficiency and scalability beyond traditional attention. Originally designed for auto-regressive tasks, its 1D structure posed challenges for 2D vision. VMamba [16] extended Mamba with cross-scan and cross-merge operations to capture pixels in all directions, creating four replicas of the S6 blocks. ViM [36] introduced bidirectional SSMs, creating forward and backward blocks to better capture LRD in images, enabling effective visual representation learning. These adaptations demonstrate that SSMs can provide an efficient alternative to ViTs, but at the cost of architectural complexity. However, integrat-

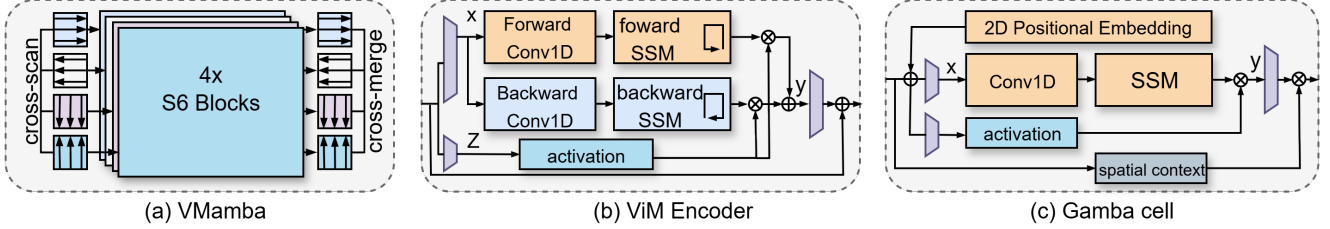


Figure 3. Schematic comparison of the proposed Gamba cell block (c): (a) VMamba block [16], and (b) ViM block [36]. Our approach introduces a single SSM layer that can directly replace the  $3 \times 3$  conv. in a standard CNN bottleneck, efficiently modeling LRD. In contrast, VMamba requires four replicas of the SSM per block, and ViM requires two replicas.

ing SSMs into standard CNN pipelines remains challenging. Existing SSM-based models require heavy preprocessing such as cross-scan, cross-merge, or bidirectional replication, resulting in multiple SSM instances per block and increased architectural complexity, see Fig. 3.

To achieve a balance between efficiency and simplicity, it becomes essential to explore lightweight mechanisms that can embed sequence modeling within CNN backbones without architectural overhead. Inspired by Bottleneck Transformers [26], which successfully incorporate MHSA into CNN, we aim to bring SSM into CNN pipelines in a similarly efficient and modular manner.

### 3. Preliminaries

#### 3.1. SSM

SSM represents an input sequence  $x(t) \in \mathbb{R}$  through a latent state  $h(t) \in \mathbb{R}^N$  using the following continuous linear system:

$$\begin{aligned} h'(t) &= Ah(t) + Bx(t), \\ y(t) &= Ch(t) + Dx(t), \end{aligned} \quad (1)$$

where  $A \in \mathbb{R}^{N \times N}$  is the state transition matrix,  $B \in \mathbb{R}^{N \times 1}$  maps the input to the state,  $C \in \mathbb{R}^{1 \times N}$  maps the state to the output, and  $D \in \mathbb{R}$  is a feedthrough term.

To apply SSMs in deep learning, the continuous system is discretized using the Zero-Order Hold (ZOH) method, which assumes the input remains constant over each time step  $\Delta t$ . The discretized system is defined as:

$$\hat{A} = e^{A\Delta t}, \quad \hat{B} = \left( \int_0^{\Delta t} e^{A\tau} d\tau \right) B, \quad (2)$$

leading to the discrete recurrence:

$$\begin{aligned} h_k &= \hat{A}h_{k-1} + \hat{B}x_k, \\ y_k &= Ch_k + Dx_k. \end{aligned} \quad (3)$$

Earlier deep SSM variants such as S4 introduced efficient parameterizations and fast discretization for long-range modeling. Mamba [9] extends these formulations

by making the parameters  $B$ ,  $C$ , and the discretization scale input-dependent. This dynamic adaptation allows the model to selectively retain relevant information and efficiently model LRD, achieving strong scalability and efficiency beyond traditional attention mechanisms.

## 4. Method

**Problem Statement** Existing SSM adaptations for visual tasks, such as VMamba [16] and ViM [36], rely on cross-scan, cross-merge, or bidirectional operations to capture LRD. While effective at modeling global context, these designs require multiple SSM replicas per block, significantly increasing memory usage and architectural complexity, see Fig. 3. This makes them unsuitable as drop-in replacements for the standard  $3 \times 3$  conv. in CNN bottlenecks, which are designed for efficiency, modularity, and simplicity.

**Goal** Our objective is to adapt Mamba-style SSMs to fit directly into a CNN bottleneck, replacing the  $3 \times 3$  conv. with a single forward SSM pass per block. This design aims to efficiently capture LRD within a standard CNN pipeline while maintaining low computational and memory overhead. By integrating SSMs in a modular and lightweight manner, we aim to surpass the efficiency of traditional CNN and reduce the memory demands of Bottleneck Transformers [26], whose MHSA has quadratic complexity.

### 4.1. Gamba Cell

The original Mamba model relies on causality, making it suitable for auto-regressive tasks but suboptimal for vision, where pixels are processed simultaneously. These causal constraints introduce long-range decay, weakening dependencies over distance (eqn. 3), since the  $i$ -th token depends only on the  $(i-1)$ -th token.

Therefore the Gamba cell removes this causality enabling global pixel interactions and added 2D RPE to enhance spatial awareness. Given an input feature  $X \in \mathbb{R}^{B \times C \times H \times W}$ , we reshape it to a sequence  $X_{\text{seq}} \in \mathbb{R}^{B \times (HW) \times C}$  and add RPE  $P = R_h + R_w \in \mathbb{R}^{1 \times C \times (HW)}$ ,

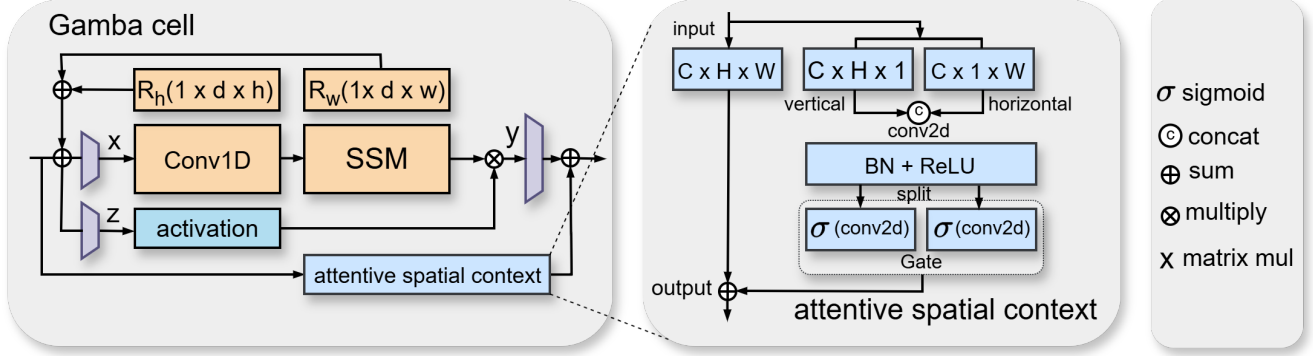


Figure 4. Gamba Bottleneck showing Gamba Cell and the ASC module.

which inject spatial priors along height and width. The enriched sequence becomes  $X_{\text{seq}} = X_{\text{seq}} + P^T$ .

Then the sequence pass through Mamba block  $M$ , which results to  $X_{\text{mamba}} = M(X_{\text{seq}})$  that captures LRD, and is then reshaped back to  $X_{\text{out}} \in \mathbb{R}^{B \times C \times H \times W}$ .

**ASC Module** While SSM captures LRD through global interactions, adding 2D-RPE alone is insufficient for precise 2D spatial modeling. To address this, we introduce ASC, a lightweight attentive module that enhances fine-grained spatial context while preserving global interactions, without the need to reapply the SSM block. Fig. 5 illustrates ASC implementation. Unlike the original Coordinate At-

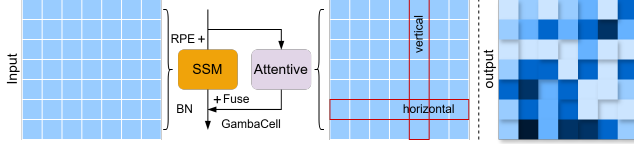


Figure 5. ASC fuses SSM and RPE to form the Gamba cell.

tention [14], which encodes spatial coordinates by separately aggregating horizontal and vertical features and fusing them uniformly, we extend this design to capture directional asymmetry and channel-dependent context sensitivity. Specifically, ASC introduces per-channel adaptive gating and axis-wise learnable biases, enabling each feature channel to dynamically balance horizontal and vertical information while encoding asymmetric spatial priors. Given an input feature  $X \in \mathbb{R}^{B \times C \times H \times W}$ , ASC performs coordinate pooling along height ( $x_h$ ) and width ( $x_w$ ), followed by shared transformations and gated fusion:

$$f_h = \text{Conv}_h(x_h) + b_h, \quad (4)$$

$$f_w = \text{Conv}_w(x_w) + b_w, \quad (5)$$

$$\text{ASC}(X) = X \odot (\alpha f_h + (1 - \alpha) f_w), \quad (6)$$

where  $\alpha \in \mathbb{R}^{1 \times C \times 1 \times 1}$  is the learnable per-channel gate,  $b_h$  and  $b_w$  are axis-wise learnable biases, and  $\odot$  denotes element-wise multiplication.

These extensions allow ASC to capture fine-grained and asymmetric spatial dependencies along both axes efficiently, improving localized context modeling without the overhead of repeated SSM blocks.

#### 4.1.1. Computation Efficiency

The Gamba block leverages SSM to capture LRD efficiently, similar to SA in Transformers. Given a visual sequence  $T \in \mathbb{R}^{1 \times M \times D}$  with default  $E = 2D$ , the computational complexities are:

$$\Omega(\text{self-attention}) = 4MD^2 + 2M^2D, \quad (7)$$

$$\Omega(\text{SSM}) = 3M(2D)N + M(2D)N, \quad (8)$$

$$\Omega(\text{CNN}) = M \cdot K^2 \cdot D^2. \quad (9)$$

Here, SA scales quadratically with sequence length  $M$ , whereas SSM scales linearly, enabling efficient processing of long sequences. Unlike CNN that capture local context efficiently, but capturing global interactions requires deeper stacks or larger RF, increasing memory and computation compared to SSM-based approaches like vGamba.

## 4.2. Architectural details

The first three stages capture local details and perform low-level feature extraction, where the input  $x \in \mathbb{R}^{C \times H \times W}$  is processed through a stem layer and standard ResNet bottleneck blocks [12]. These layers extract hierarchical features while progressively reducing spatial dimensions:

$$x_1 \in \mathbb{R}^{C_1 \times \frac{H}{4} \times \frac{W}{4}}, \quad x_2 \in \mathbb{R}^{C_2 \times \frac{H}{8} \times \frac{W}{8}}, \quad x_3 \in \mathbb{R}^{C_3 \times \frac{H}{16} \times \frac{W}{16}}$$

Stage 4, we replace the  $3 \times 3$  conv block with Gamba cell, enhancing LRD and global context modeling. The hybrid vGamba captures feature representations at deeper levels:

$$x_4 \in \mathbb{R}^{C_4 \times \frac{H}{32} \times \frac{W}{32}}$$

Finally, global average pooling (GAP) and a fully connected layer (FC) produce the final classification output:

$$y = \text{FC}(\text{GAP}(x_4))$$

#### 4.2.1. Variants

Model	GFLOP	Param	Depth	Blocks
vGamba-B	3.88G	19.45M	50	[3, 4, 6, 3]
vGamba-L	7.61G	38.44M	101	[3, 4, 23, 3]
vGamba-X	11.35G	54M	152	[3, 8, 36, 3]

Table 1. Variants of vGamba-Base, Large and XLarge

## 5. Experiments

We evaluated vGamba on ImageNet-1K for classification (Section 5.1), ADE20K for segmentation (Section 5.2), and COCO for detection (Section 5.3). Additionally, we conducted experiments on the AID dataset (Section 5.5) and performed ablation studies (Section 5.6). Experiments are conducted on NVIDIA GeForce RTX 4090 GPU, featuring 24 GB of GDDR6X VRAM, CUDA Compute Capability 8.9, and driver version 570.144 with CUDA 12.8 support.

### 5.1. Classification

**Settings.** The ImageNet-1K dataset [5] contains 1.28M training images and 50K validation images across 1,000 categories. Training follows ConvNeXt [18] settings, using augmentations like random cropping, flipping, label-smoothing, mixup, and random erasing. For  $224^2$  input images, we optimize with AdamW with momentum 0.9, batch size 64, and weight decay 0.05. Then trained vGamba models for 250 epochs with a cosine schedule and EMA, starting with a  $1 \times 10^{-3}$  learning rate. Testing includes center cropping to  $224^2$  images.

**Results.** Table (2) vGamba demonstrates a better balance of efficiency and performance on ImageNet-1K, with vGamba-B achieving 81.1% Top-1 accuracy using only 3.7G FLOP and 18.9M parameters. Compared to classical CNNs, ResNet-50 reaches 76.2% with higher FLOPs (3.9G) and more parameters (25M), while attention-based BoT50 improves accuracy to 78.3% with fewer parameters (20.8M). Transformer-based models like ViM-S achieve 80.3% at 5.3G FLOPs, and hybrid architectures such as VMamba-T and MambaVision-T push accuracy further to 82.6% and 82.3% respectively, but at higher compute costs. Overall, vGamba achieves competitive accuracy with lower computational cost and smaller model size.

### 5.2. Segmentation

**Settings.** We conducted semantic segmentation experiments using the ADE20K dataset [35] within the UperNet

Table 2. Model performance comparison on ImageNet-1K.

Method	IMAGENET-1K			
	Size	FLOPs (G)	Param (M)	Top-1 (%)
ResNet-50 [12]	$224^2$	3.9G	25M	76.2%
ResNet-101 [12]	$224^2$	7.6G	45M	77.4%
ResNet-152 [12]	$224^2$	11.3G	60M	78.3%
BoT50 [26]	$224^2$	-	20.8M	78.3%
EffNet-B2 [28]	$224^2$	1.0G	9M	80.1%
EffNet-B3 [28]	$300^2$	1.8G	12M	81.6%
RegNetY-4GF [24]	$224^2$	4.0G	21M	80.0%
RegNetY-8GF [24]	$224^2$	8.0G	39M	81.7%
ViT-B/16 [7]	$384^2$	55.4G	86M	77.9%
ViT-L/16 [7]	$384^2$	190.7G	307M	76.5%
DeiT-S [29]	$224^2$	4.6G	22M	79.8%
DeiT-B [29]	$224^2$	17.5G	86M	81.8%
Swin-T [17]	$224^2$	4.5G	29M	81.3%
CoaT-Lite-S [4]	$224^2$	4.1G	19.8M	82.3%
CrossViT-B [1]	$240^2$	20.1G	105.0M	82.2%
Vim-S [36]	$224^2$	5.3G	26M	80.3%
Vim-B [36]	$224^2$	-	98M	81.9%
EffVMamba-T [22]	$224^2$	0.8G	6M	76.5%
EffVMamba-S [22]	$224^2$	1.3G	11M	78.7%
S4ND-ViT-B [21]	$224^2$	17.1G	89M	80.4%
VMamba-T [16]	$224^2$	4.9G	30M	82.6%
MambaVision-T [11]	$224^2$	4.4G	31.8M	82.3%
vGamba-B	$224^2$	3.7G	18.9M	81.1%
vGamba-L	$224^2$	6.3G	31.8M	82.8%
vGamba-X	$224^2$	11.3G	54M	83.2%

framework [32]. The backbone network was initialized with pre-trained weights from ImageNet-1K [5], while the remaining components were randomly initialized. Model optimization was performed using the AdamW optimizer with a batch size of 16. The model was trained for 160k iterations to ensure thorough learning.

**Results.** Table (3), vGamba achieves state-of-the-art performance in semantic segmentation on ADE20K, outperforming both CNNs and Transformer-based models while maintaining computational efficiency. Its ability to effectively model long-range dependencies and spatial coherence enables better segmentation accuracy with lower computational overhead compared to ViT. vGamba-L achieves the highest mIoU of 51.4 (SS) and 52.2 (MS), surpassing vGamba-B (50.9, 51.3) and Swin-B (48.1, -). Similarly, vGamba-B maintains good performance at 50.9 (SS) and 51.3 (MS) with fewer parameters than larger ViTs. These results establish vGamba as a highly effective alternative for semantic segmentation, offering a balance of accuracy and efficiency that makes it good for real-world applications.

Table 3. Comparison of semantic segmentation results on ADE20K using UperNet. FLOPs are measured with an input size of 512×2048.

ADE20K				
Backbone	Param (M)	FLOP (G)	mIoU (SS)	mIoU (MS)
ResNet-50 [12]	67	953	42.1	42.8
ResNet-101 [12]	85	1030	42.9	44.0
ConvNeXt-T [18]	60	939	46.0	46.7
ConvNeXt-S [18]	82	1027	48.7	49.6
DeiT-S + MLN [29]	58	1217	43.8	45.1
DeiT-B + MLN [29]	144	2007	45.5	47.2
Swin-T [17]	60	945	44.5	45.8
Swin-S [17]	81	1039	47.6	49.5
Swin-B [17]	121	1188	48.1	-
Vim-S [36]	46	-	44.9	-
VMamba-T [16]	62	949	47.9	48.8
VMamba-S [16]	82	1028	50.6	51.2
VMamba-B [16]	122	1170	51.0	51.6
EfficientVMamba-T [22]	14	230	38.9	39.3
EfficientVMamba-S [22]	29	505	41.5	42.1
EfficientVMamba-B [22]	65	930	46.5	47.3
vGamba-B	55	941	50.9	51.3
vGamba-L	71	1019	51.4	52.2

### 5.3. Object Detection

**Settings.** We evaluated our model on object detection and instance segmentation tasks using the COCO 2017 dataset [15], which consists of approximately 118K training images and 5K validation images. vGamba was utilized as the backbone and integrated into the Mask R-CNN framework [13] for feature extraction. The model was initialized with weights pre-trained on ImageNet-1K (300 epochs) and trained for 12 epochs (1×) and 36 epochs (3×).

**Results** Table (4) The comparison of vGamba with other models in Mask R-CNN and Cascade Mask R-CNN detection tasks reveals notable performance.

- In the Mask R-CNN 1× schedule, vGamba-B achieves an  $AP_b$  of 44.9 and  $AP_m$  of 42.0, with lower FLOPs (225G) and fewer parameters (49M) compared to other models. The larger vGamba-L improves to 49.8 and 45.3 for  $AP_b$  and  $AP_m$ , respectively, while having good computational requirements.
- In the Mask R-CNN 3× MS schedule, vGamba-L demonstrates impressive performance with  $AP_b$  at 51.3 and  $AP_m$  at 46.1, surpassing several larger models like Swin-S and ConvNeXt-S in terms of both accuracy and efficiency.
- For Cascade Mask R-CNN 3× MS schedule, vGamba-B outperforms models like Swin-T and ConvNeXt-T with

Table 4. Cascade Mask R-CNN detection results.

Backbone	FLOPs (G)	Params (M)	$AP_b$	$AP_m$
<b>Mask R-CNN 1× schedule</b>				
Swin-T [17]	267G	48M	42.7	39.3
ConvNeXt-T [18]	262G	48	44.2	40.1
VMamba-T [16]	271G	50	47.3	42.7
Swin-S [17]	354G	69	44.8	40.9
ConvNeXt-S [18]	348G	70	45.4	41.8
VMamba-S [16]	349G	70	48.7	43.7
Swin-B [17]	496G	107	46.9	42.3
ConvNeXt-B [18]	486G	108	47.0	42.7
VMamba-B [16]	485G	108	49.2	44.1
vGamba-B	225G	49	44.9	42.0
vGamba-L	254G	71	49.8	45.3
<b>Mask R-CNN 3× MS schedule</b>				
Swin-T [17]	267G	48	46.0	41.6
ConvNeXt-T [18]	262G	48	46.2	41.7
VMamba-T [16]	271G	50	48.8	43.7
Swin-S [17]	354G	69	48.2	43.2
ConvNeXt-S [18]	348G	70	47.9	42.9
VMamba-S [16]	349G	70	49.9	44.2
vGamba-L	254G	71	51.3	46.1
<b>Cascade Mask R-CNN 3× MS schedule</b>				
DeiT-Small/16 [29]	889G	80	48.0	41.4
ResNet-50 [12]	739G	82	46.3	40.1
Swin-T [17]	745G	86	50.4	43.7
ConvNeXt-T [18]	741G	86	50.4	43.7
MambaVision-T [11]	740G	86	51.0	44.3
Swin-S [17]	838G	107	51.9	45.0
ConvNeXt-S [18]	827G	108	51.9	45.0
MambaVision-S [11]	828G	108	52.1	45.2
Swin-B [17]	982G	145	51.9	45.0
ConvNeXt-B [18]	964G	146	52.7	45.6
MambaVision-B [11]	964G	145	52.8	45.7
vGamba-B	727G	76	50.8	43.7
vGamba-L	905G	123	53.1	46.3

an  $AP_b$  of 50.8 and  $AP_m$  of 43.7. The larger vGamba-L performs similarly to the top-performing models, achieving 53.1 for  $AP_b$  and 46.3 for  $AP_m$ , with fewer computational resources than some alternatives.

### 5.4. Scaling Performance

We evaluate the scaling performance of ResNet-50, BoT-Net, and vGamba backbones with FPN for downstream tasks. We examine FPS and memory usage change with 512, 640, and 1024 resolutions. This provides insight into each model’s efficiency and practical suitability across different computational budgets and image sizes. See Figure 6.

Table 5. Gamba bottleneck analysis

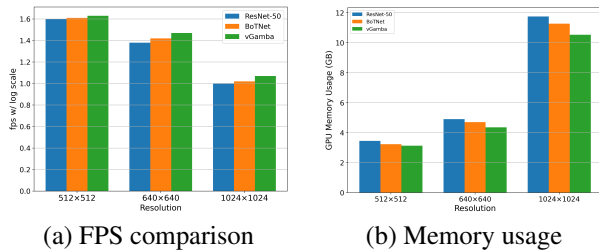


Figure 6. Scaling performance of ResNet-50, BoTNet, and vGamba with FPN across different input resolutions.

vGamba consistently outperforms ResNet-50 and BoTNet in both memory usage and inference speed across all resolutions. At  $1024^2$ , it uses 10.53 GB of GPU memory, roughly 10% less than ResNet-50 (11.75 GB), while achieving higher log-scaled FPS (1.07 vs. 1.00–1.02), corresponding to a 3–6% speedup. These results highlight vGamba’s efficient trade-off between speed and memory.

## 5.5. Additional Experiments

We performed qualitative experiments using Hi-Res Grad-CAM [8] on the AID aerial dataset [31] due to its inherent long-range dependencies to analyze the model’s decision-making. The visualized attention highlights both local features and broader context, such as runway layouts and surrounding infrastructure, demonstrating the model’s ability to capture long-range dependencies in complex aerial scenes. These results confirm the model’s effectiveness and explainability for aerial scene understanding, Fig. 7.

**Effective Receptive Field (ERF)** The ERF quantifies how much of the input image effectively contributes to an output activation, revealing how models capture LRD beyond their theoretical receptive field [19]. We compare ResNet-50, BotNet, and vGamba after training under identical settings.

As shown in Fig. 8, ResNet-50 exhibits local ERFs, indicating CNNs primarily capture nearby spatial context. BotNet shows global receptive coverage due to its attention mechanism, while vGamba achieves comparable global context with better efficiency through its SSM-based design. ERFs remain local in layers 0–3 but become global in layer 4, validating our replacement of the final bottleneck with the Gamba cell for efficient LRD modeling.

## 5.6. Ablation

### 5.6.1. Effects of components

We determine the contribution of each component in vGamba. We removed each components and analyze their effects on accuracy and efficiency. Although we observed

Model (components)	Size	Top-1	FLOP	Param
w/o RPE	$224^2$	80.2%	3.7G	18.9M
w/ RPE	$224^2$	80.5%	3.7G	18.9M
w/o ASC	$224^2$	80.3%	3.7G	18.8M
w/ ASC	$224^2$	81.1%	3.7G	18.9M

very minimal changes to the model complexities when either we removed RPE or ASC module.

**Results.** Specifically, we observed +0.3% in accuracy when we added RPE and also +0.8% for adding ASC module while maintaining efficiency (similar FLOP and parameter count).

## 6. Conclusion

This work advances bottleneck design for LRD modeling by showing that a single, lightweight SSM-enhanced bottleneck can effectively replace both CNN and Transformer bottlenecks for efficient global context modeling. While ResNet bottlenecks remain limited by their local receptive fields and Transformer bottlenecks incur high computational cost, the proposed Gamba bottleneck bridges this gap by embedding a spatially aware SSM (the Gamba cell) and the ASC module into a compact structure that preserves efficiency without sacrificing representational strength. The resulting backbone, vGamba, consistently captures LRD more accurately than CNN-based and Transformer-based alternatives while maintaining lower memory and FLOPs. Across classification, detection, and segmentation, vGamba shows better performance and smoother LRD convergence. vGamba offers a practical, scalable alternative to existing visual backbones.

### 6.1. Limitations

Despite the promising results, this work has several limitations. First, although vGamba effectively captures long-range dependencies, it remains sensitive to hyperparameter choices. Adapting these settings to different vision tasks may require additional tuning and can lead to performance variability.

Additionally, while vGamba performs strongly on standard benchmarks, its effectiveness in highly complex or domain-specific tasks—such as those requiring extreme precision (e.g., medical imaging)—has not been evaluated. Future work should explore these settings and further optimize the model’s computational efficiency for broader applicability.

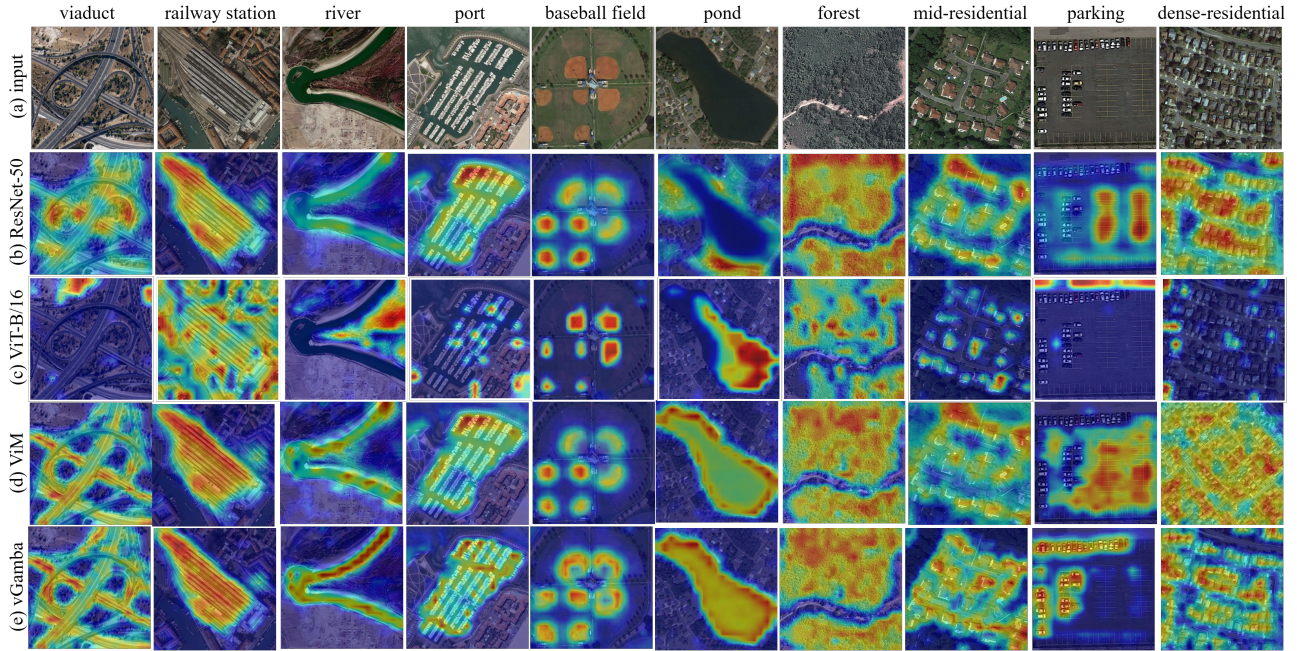


Figure 7. Hi-Res CAM visualization on the Aerial Image dataset, highlighting model decision regions through heatmaps

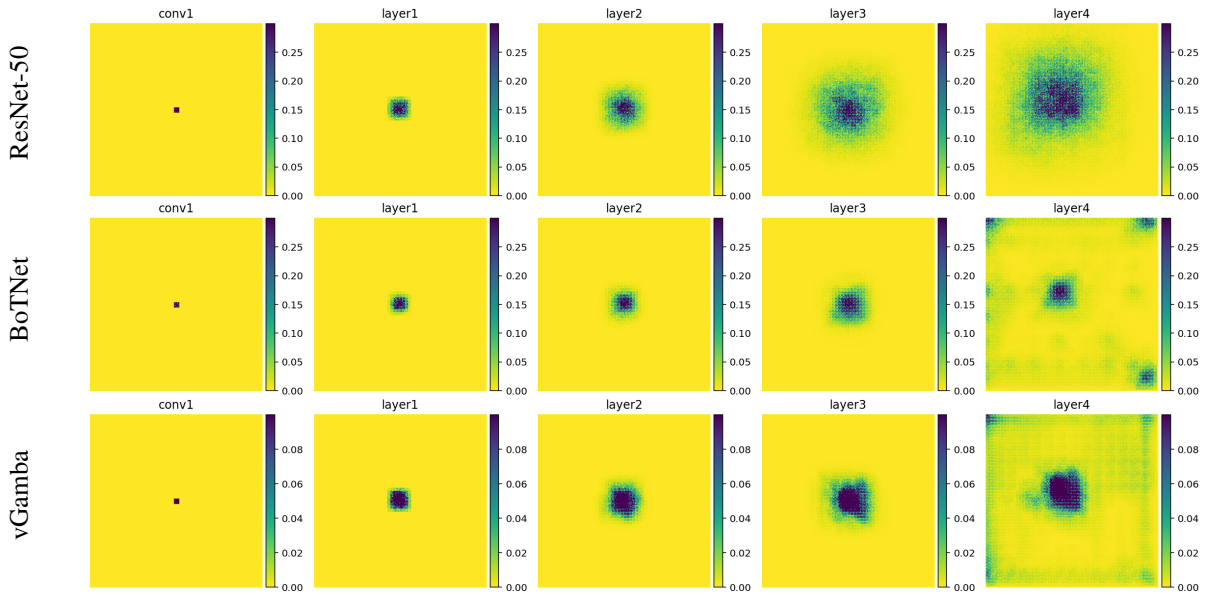


Figure 8. ERF comparison among ResNet-50, BoTNet, and vGamba across layers.

## 6.2. Broader Impact

vGamba model, with its efficient capture of long-range dependencies, has broad applications across healthcare (e.g., medical image analysis for tumor detection), autonomous driving (enhancing object detection in complex environments), robotics (improving visual perception for navigation and manipulation), and aerial vision (optimizing analysis of surveillance and environmen-

tal monitoring). Its ability to process high-resolution images efficiently makes vGamba a valuable tool for real-time vision systems across diverse industries.

## References

- [1] Chun-Fu Richard Chen, Quanfu Fan, and Rameswar Panda. Crossvit: Cross-attention multi-scale vision transformer for image classification. In *Proceedings of the IEEE/CVF International Conference on Computer Vision*, pages 357–366, 2021. 5
- [2] Xuanyao Chen, Zhijian Liu, Haotian Tang, Li Yi, Hang Zhao, and Song Han. Sparsevit: Revisiting activation sparsity for efficient high-resolution vision transformer. In *Proceedings of the IEEE/CVF Conference on Computer Vision and Pattern Recognition*, pages 2061–2070, 2023. 1, 2
- [3] François Chollet. Xception: Deep learning with depthwise separable convolutions. In *Proceedings of the IEEE conference on computer vision and pattern recognition*, pages 1251–1258, 2017. 1
- [4] Zihang Dai, Hanxiao Liu, Quoc V. Le, and Mingxing Tan. Coatnet: Marrying convolution and attention for all data sizes. In *Advances in Neural Information Processing Systems*, pages 3965–3977, 2021. 5
- [5] Jia Deng, Wei Dong, Richard Socher, Li-Jia Li, Kai Li, and Li Fei-Fei. Imagenet: A large-scale hierarchical image database. In *2009 IEEE conference on computer vision and pattern recognition*, pages 248–255. Ieee, 2009. 5
- [6] Xiaohan Ding, Xiangyu Zhang, Jungong Han, and Guiguang Ding. Scaling up your kernels to 31x31: Revisiting large kernel design in cnns. In *Proceedings of the IEEE/CVF Conference on Computer Vision and Pattern Recognition (CVPR)*, pages 11963–11975, 2022. 1
- [7] Alexey Dosovitskiy, Lucas Beyer, Alexander Kolesnikov, Dirk Weissenborn, Xiaohua Zhai, Thomas Unterthiner, Mostafa Dehghani, Matthias Minderer, Georg Heigold, Sylvain Gelly, Jakob Uszkoreit, and Neil Houlsby. An image is worth 16x16 words: Transformers for image recognition at scale. In *ICLR*, 2021. 1, 2, 5
- [8] Rachel Lea Draelos and Lawrence Carin. Use hirescam instead of grad-cam for faithful explanations of convolutional neural networks. *arXiv preprint arXiv:2011.08891*, 2020. 7
- [9] Albert Gu and Tri Dao. Mamba: Linear-time sequence modeling with selective state spaces. *arXiv preprint arXiv:2312.00752*, 2023. 1, 2, 3
- [10] Albert Gu, Karan Goel, and Christopher Ré. Efficiently modeling long sequences with structured state spaces. *arXiv preprint arXiv:2111.00396*, 2021. 1
- [11] Ali Hatamizadeh and Jan Kautz. Mambavision: A hybrid mamba-transformer vision backbone. *arXiv preprint arXiv:2407.08083*, 2024. 5, 6
- [12] Kaiming He, Xiangyu Zhang, Shaoqing Ren, and Jian Sun. Deep residual learning for image recognition. In *Proceedings of the IEEE conference on computer vision and pattern recognition*, pages 770–778, 2016. 1, 4, 5, 6
- [13] Kaiming He, Georgia Gkioxari, Piotr Dollár, and Ross Girshick. Mask r-cnn. In *Proceedings of the IEEE International Conference on Computer Vision (ICCV)*, pages 2961–2969, 2017. 6
- [14] Qibin Hou, Daquan Zhou, and Jiashi Feng. Coordinate attention for efficient mobile network design. In *Proceedings of the IEEE/CVF Conference on Computer Vision and Pattern Recognition (CVPR)*, pages 13713–13722, 2021. 4
- [15] Tsung-Yi Lin, Michael Maire, Serge Belongie, James Hays, Pietro Perona, Deva Ramanan, Piotr Dollár, and C. Lawrence Zitnick. Microsoft coco: Common objects in context. In *Computer Vision—ECCV 2014: 13th European Conference, Zurich, Switzerland, September 6–12, 2014, Proceedings, Part V*, pages 740–755. Springer International Publishing, 2014. 6
- [16] Yue Liu, Yunjie Tian, Yuzhong Zhao, Hongtian Yu, Lingxi Xie, Yaowei Wang, Qixiang Ye, Jianbin Jiao, and Yunfan Liu. Vmamba: Visual state space model. *Advances in neural information processing systems*, 37:103031–103063, 2025. 1, 2, 3, 5, 6
- [17] Ze Liu, Yutong Lin, Yue Cao, Han Hu, Yixuan Wei, Zheng Zhang, Stephen Lin, and Baining Guo. Swin transformer: Hierarchical vision transformer using shifted windows. In *Proceedings of the IEEE/CVF International Conference on Computer Vision*, pages 10012–10022, 2021. 5, 6
- [18] Zhuang Liu, Hanzi Mao, Chao-Yuan Wu, Christoph Feichtenhofer, Trevor Darrell, and Saining Xie. A convnet for the 2020s. In *Proceedings of the IEEE/CVF Conference on Computer Vision and Pattern Recognition*, pages 11976–11986, 2022. 5, 6
- [19] Wenjie Luo, Yujia Li, Raquel Urtasun, and Richard Zemel. Understanding the effective receptive field in deep convolutional neural networks. In *Advances in Neural Information Processing Systems (NeurIPS)*, 2016. 7
- [20] Xuezhe Ma, Xiang Kong, Sinong Wang, Chunting Zhou, Jonathan May, Hao Ma, and Luke Zettlemoyer. Luna: Linear unified nested attention. pages 2441–2453, 2021. 1, 2
- [21] Eric Nguyen, Karan Goel, Albert Gu, Gordon Downs, Preey Shah, Tri Dao, Stephen Baccus, and Christopher Ré. S4nd: Modeling images and videos as multidimensional signals with state spaces. In *Advances in Neural Information Processing Systems*, pages 2846–2861, 2022. 5
- [22] Xiaohuan Pei, Tao Huang, and Chang Xu. Efficientvmamba: Atrous selective scan for light weight visual mamba. *arXiv preprint arXiv:2403.09977*, 2024. 5, 6
- [23] Chao Peng, Xiangyu Zhang, Gang Yu, Guiming Luo, and Jian Sun. Large kernel matters – improve semantic segmentation by global convolutional network. In *Proceedings of the IEEE Conference on Computer Vision and Pattern Recognition (CVPR)*, pages 4353–4361, 2017. 2
- [24] Ilija Radosavovic, Raj Prateek Kosaraju, Ross Girshick, Kaiming He, and Piotr Dollár. Designing network design spaces. In *Proceedings of the IEEE/CVF conference on computer vision and pattern recognition*, pages 10428–10436, 2020. 1, 5
- [25] Jeong-geun Song. Ufo-vit: High performance linear vision transformer without softmax. *arXiv preprint arXiv:2109.14382*, 2021. 1, 2
- [26] Aravind Srinivas, Tsung-Yi Lin, Niki Parmar, Jonathon Shlens, Pieter Abbeel, and Ashish Vaswani. Bottleneck transformers for visual recognition. In *Proceedings of the IEEE/CVF Conference on Computer Vision and Pattern Recognition*, pages 16519–16529, 2021. 2, 3, 5

- [27] Christian Szegedy, Wei Liu, Yangqing Jia, Pierre Sermanet, Scott Reed, Dragomir Anguelov, Dumitru Erhan, Vincent Vanhoucke, and Andrew Rabinovich. Going deeper with convolutions. In *Proceedings of the IEEE conference on computer vision and pattern recognition*, pages 1–9, 2015. [1](#)
- [28] Mingxing Tan and Quoc Le. Efficientnet: Rethinking model scaling for convolutional neural networks. In *International conference on machine learning*, pages 6105–6114, 2019. [1](#), [5](#)
- [29] Hugo Touvron, Matthieu Cord, Matthijs Douze, Francisco Massa, Alexandre Sablayrolles, and Hervé Jégou. Training data-efficient image transformers & distillation through attention. In *International Conference on Machine Learning*, pages 10347–10357. PMLR, 2021. [5](#), [6](#)
- [30] Xiaolong Wang, Ross Girshick, Abhinav Gupta, and Kaiming He. Non-local neural networks. In *Proceedings of the IEEE conference on computer vision and pattern recognition*, pages 7794–7803, 2018. [2](#)
- [31] Gui-Song Xia, Jingwen Hu, Fan Hu, Baoguang Shi, Xiang Bai, Yanfei Zhong, Liangpei Zhang, and Xiaoqiang Lu. Aid: A benchmark data set for performance evaluation of aerial scene classification. *IEEE Transactions on Geoscience and Remote Sensing*, 55(7):3965–3981, 2017. [7](#)
- [32] Tete Xiao, Yingcheng Liu, Bolei Zhou, Yuning Jiang, and Jian Sun. Unified perceptual parsing for scene understanding. In *Proceedings of the European Conference on Computer Vision (ECCV)*, pages 418–434, 2018. [5](#)
- [33] Yuedong Yang, Hung-Yueh Chiang, Guihong Li, Diana Marculescu, and Radu Marculescu. Efficient low-rank backpropagation for vision transformer adaptation. 2024. [1](#), [2](#)
- [34] Fisher Yu, Vladlen Koltun, and Thomas Funkhouser. Dilated residual networks. In *Proceedings of the IEEE conference on computer vision and pattern recognition*, pages 472–480, 2017. [1](#), [2](#)
- [35] Bolei Zhou, Hang Zhao, Xavier Puig, Tete Xiao, Sanja Fidler, Adela Barriuso, and Antonio Torralba. Semantic understanding of scenes through the ade20k dataset. *International Journal of Computer Vision*, 127:302–321, 2019. [5](#)
- [36] Lianghai Zhu, Bencheng Liao, Qian Zhang, Xinlong Wang, Wenyu Liu, and Xinggang Wang. Vision mamba: Efficient visual representation learning with bidirectional state space model. *arXiv*, 2024. [1](#), [2](#), [3](#), [5](#), [6](#)